Raman and photoacoustic infrared spectra of fluorene derivatives: Experiment and calculations

K H Michaelian, S A Oladepo, J M Shaw, X Liu, Isabelle Baraille, Didier Bégué

Vibrational Spectroscopy 74 (2014) 33–46

Contents lists available at ScienceDirect

Vibrational Spectroscopy

journal homepage: www.elsevier.com/locate/vibspec

Raman and photoacoustic infrared spectra of fluorene derivatives: Experiment and calculations

K.H. Michaelian[a,*], S.A. Oladepo[a], J.M. Shaw[b], X. Liu[c], D. Bégué[d], I. Baraille[d]

[a] Natural Resources Canada, CanmetENERGY, One Oil Patch Drive, Devon, Alberta T9G 1A8, Canada
[b] Department of Chemical and Materials Engineering, University of Alberta, Edmonton, Alberta T6G 2G6, Canada
[c] Canadian Light Source Inc., 44 Innovation Boulevard, Saskatoon, Saskatchewan S7N 2V3, Canada
[d] Institut des Sciences Analytiques et de Physico-Chimie pour l'Environnement et pour les Matériaux, UMR 5254-CNRS, Equipe de Chimie Physique, Université de Pau et des Pays de l'Adour, 2 Avenue du Président Angot, 64053 Pau Cedex 9, France

ARTICLE INFO

Article history:
Received 17 February 2014
Received in revised form 7 July 2014
Accepted 11 July 2014
Available online 21 July 2014

Keywords:
Raman spectroscopy
Photoacoustic infrared spectroscopy
Aromatic hydrocarbons
DFT calculations
Variational calculations

ABSTRACT

Raman and photoacoustic (PA) infrared spectra of fluorene and four derivatives (2,3-benzofluorene, 2-methylfluorene, 2-ethylfluorene and 1,8-dimethylfluorene) were recorded and analyzed in this investigation. Mid- and far-infrared PA spectra were examined from about 2000 to 100 cm^{-1}. The Raman spectra spanned the same wavenumber range. Observed bands in both PA and Raman spectra were compared with DFT (harmonic) and variational (anharmonic) calculations, and with published spectra. The DFT calculations provided single-molecule frequencies, whereas the variational method yielded results for both monomeric and dimeric species. Many previously unknown bands, including numerous features due to combination and overtone transitions, were identified and assigned in this work.

1. Introduction

Photoacoustic (PA) infrared spectra of tetracene ($C_{18}H_{12}$), pentacene ($C_{22}H_{14}$), perylene ($C_{20}H_{12}$) and pyrene ($C_{16}H_{10}$) were recently obtained in our laboratory and interpreted in light of density functional theory (DFT) calculations [1,2]. The "fingerprint" and far-infrared regions (together, approximately 2000–80 cm^{-1}) were studied in detail in these investigations. In addition to the predicted infrared-active bands, the PA spectra of these hydrocarbons display many features due to overtones and combinations. Moreover, numerous Raman-active (*gerade*) vibrations also give rise to bands in the PA spectra, which thus convey considerable information regarding the structures of these compounds.

Vibrational spectra of these, and related similar, aromatic hydrocarbons are important in two quite different contexts and both contexts motivate the present work. The first, relevant to the utilization of certain hydrocarbon feed stocks, is the need for characterization of asphaltenes. These complex and highly aromatic species arise in numerous hydrocarbon resources and are particularly abundant in bitumen derived from oil sands, heavy oils, and similar substances. While asphaltenes are generally believed to consist of extended aromatic ring systems, aliphatic chains, and heteroatoms (sulphur, nitrogen and oxygen), their structural details remain the subject of much discussion and debate. Infrared and Raman spectra of asphaltenes and representative model compounds (together with other spectroscopic and non-spectroscopic analyses) are expected to provide critical information pertaining to this question. For this reason, acquisition and interpretation of vibrational spectra are key components of an ongoing research program in our laboratory. Related previous work combined spectroscopy with the determination of thermophysical properties of similar aliphatic and aromatic hydrocarbons [3,4]. The second originates in astrophysics and astrochemistry, where infrared absorption spectra of aromatic hydrocarbons and various forms of elemental carbon are frequently invoked in comparisons with emission spectra from the interstellar medium. The extensive detail in PA infrared spectra of aromatic hydrocarbons—particularly in the 2000–1700 cm^{-1} and higher wavenumber regions—enables observation of little-known combination bands involving C—H out-of-plane vibrations and other modes [2,5–7]. These results can also be used to investigate mechanical and electrical anharmonicities of the vibrations, a topic that is incorporated into our research for the first time in the present work. With regard to the astrophysical context, it should be noted that we consider only neutral species in our studies; this contrasts with other investigations where both

* Corresponding author. Tel.: +1 780 987 8646; fax: +1 780 987 8676.
E-mail addresses: Kirk.Michaelian@NRCan-RNCan.gc.ca, michaeli@nrcan.gc.ca (K.H. Michaelian).

http://dx.doi.org/10.1016/j.vibspec.2014.07.003
0924-2031/

positive and negative ions were included in laboratory simulations of interstellar spectra [7–15]. For both hydrocarbon resource characterization and astrophysics applications, low wavenumber Raman and PA spectra may also permit identification of particular compounds or sub-molecular aromatic motifs in mixtures because at low wavenumbers spectra are less complex and bands are often linked to specific large-scale structures present in molecules, and specific molecular interactions. Concurrent experimental and computational evaluation of spectra for "families" of compounds provides a productive basis for gaining insights into both applications in general and into the identification of specific constituents in mixtures.

Raman and PA infrared spectra of fluorene ($C_{13}H_{10}$; also known as 9*H*-fluorene or diphenylenemethane), 2,3-benzofluorene ($C_{17}H_{12}$), 2-methylfluorene ($C_{14}H_{12}$), 2-ethylfluorene ($C_{15}H_{14}$), and 1,8-dimethylfluorene ($C_{15}H_{14}$) were acquired in the present work. Raman spectra were obtained in the wavenumber range from about 2000 to 100 cm^{-1}, while far- and mid-infrared PA spectra together spanned the same region. Harmonic and anharmonic wavenumber calculations were also performed for these compounds. The observed Raman and infrared bands are correlated with calculated fundamental vibrations, or alternatively with predicted overtone and combination transitions, in this article. These results are expected to significantly enhance knowledge of the vibrational spectra of fluorene and its derivatives.

2. Frequency calculations

Calculations of frequencies and the corresponding intensities of large molecules according to harmonic theory are in general sufficiently reliable to enable analysis of the spectra and this strategy was employed in our earlier work [1,2]. Nevertheless, the results provided by the standard double-harmonic (mechanical and electrical) approximation are not sufficiently accurate for fine spectroscopic assignments. The appearance of combination and overtone bands in the PA spectra of aromatic hydrocarbons also shows that the harmonic approximation should be augmented by another approach. Accordingly, both harmonic (DFT) and anharmonic (variational) calculations were carried out in the present investigation.

2.1. DFT method

Fundamental frequencies were predicted at the B3LYP/6-311+G(d,p) level of theory as implemented in the Gaussian 09 suite of programs. Infrared and Raman frequencies and intensities were obtained in these calculations. Only results indicating energy minima with positive frequencies are reported. Basis sets were sufficiently large to ensure reasonable accuracies of the predicted frequencies. Calculated intensities were taken into consideration when correlating experimental data with the predicted bands for each compound.

2.2. Variational method

As mentioned above, the occurrence of combination and overtone bands in the hydrocarbon spectra indicates the anharmonic nature of the vibrations. Some authors scale their DFT-calculated frequencies to allow for anharmonicity and to obtain better agreement with the experimental data, even though this approach does not account for overtones or combination bands. Further the presence of anharmonic bands in the infrared spectra is a manifestation of the breakdown of the double-harmonic approximation. Since both mechanical (anharmonicity of the potential) and electrical (non-linear dependence of the dipole moment on the normal coordinates) anharmonicities are expected to give intensity to non-fundamental transitions, these two effects should be considered explicitly in the treatment of transition energies and related vibrational wavefunctions.

In this work frequency calculations were carried out in the mechanical and electrical anharmonic approximations, in the same process, using the variational method developed by Bégué et al. [16–20] and Baraille et al. [21], implemented in the P_Anhar.v2.0 program [22]. All vibrational frequencies (fundamentals, combination bands and overtones) that contribute to the infrared and Raman spectra, including those due to torsional motion, were computed. Calculations were performed for monomers and dimers of each compound.

3. Experimental

Fluorene, 2,3-benzofluorene, 2-methylfluorene, 2-ethylfluorene and 1,8-dimethylfluorene were obtained from commercial sources at purity levels of at least 98% and analyzed as received. In some cases, samples were ground manually prior to acquisition of their spectra.

3.1. Raman spectra

Raman spectra were obtained using two spectrometers at CanmetENERGY (Devon, Alberta). In one set of experiments, a Renishaw InVia microscope-based system was coupled to a Spectra Physics 125 He–Ne laser, which provided excitation at 633 nm. Several milligrams of each solid were examined with the use of a 50× microscope objective. Spectra were acquired with a spherically focused incident beam; typical resolution was better than 2 cm^{-1}. Total accumulation time was 5 min for each spectrum. The other group of experiments was performed with a Bruker IFS 88 FT spectrometer and FRA 106 Raman accessory. Excitation of the FT-Raman spectra was effected with a 1064-nm Nd:YAG laser at power levels between 90 and 260 mW. Ten 32-scan spectra with a resolution of 4 cm^{-1} were averaged for each sample.

3.2. Far-infrared spectra

PA far-infrared spectra were acquired at a resolution of 6 cm^{-1} using two different Bruker IFS 66v/S Fourier transform infrared (FT-IR) spectrometers. This resolution, which is somewhat lower than that utilized with other infrared techniques, was found to be adequate for the present study. Higher resolution yielded poorer signal-to-noise ratios and is unnecessary in view of the widths of the PA bands, which tend to be greater than those in the corresponding Raman spectra. The first instrument, at CanmetENERGY, was operated in both rapid- and step-scan modes. The He–Ne laser modulation frequency was 1.6 kHz for the rapid-scan measurements, corresponding to the lowest scan velocity of this instrument. Large amplitude phase modulation [1] was employed in the step-scan experiments, with a Signal Recovery lock-in amplifier being utilized for demodulation. The second spectrometer was located at the Canadian Light Source (Saskatoon, Saskatchewan). Rapid-scan spectra were acquired under conditions similar to those just mentioned. A thermal (globar) source was employed with this instrument.

Standard MTEC 300 gas-microphone PA accessories were used with both spectrometers; the sample cells were fitted with polyethylene windows. Helium was employed as the carrier gas. Multilayer mylar beamsplitters were installed in the interferometers. Spectra were recorded between about 700 and 50 cm^{-1}, due to limits imposed by the optical materials. Carbon black powder or an MTEC carbon black reference yielded reference spectra that were

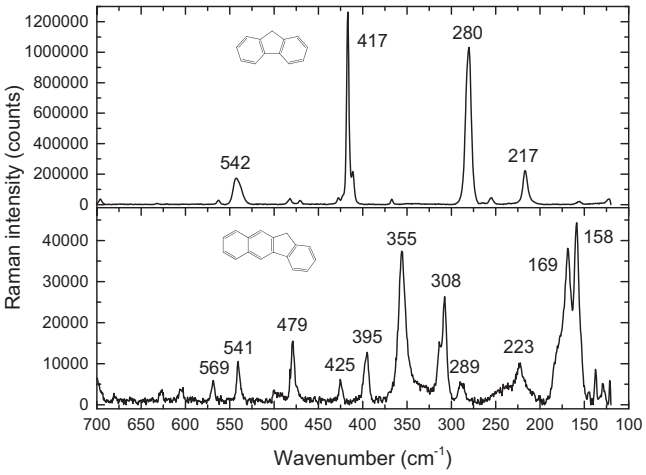

Fig. 1. Low wavenumber Raman spectra of fluorene (top panel) and 2,3-benzofluorene (bottom panel).

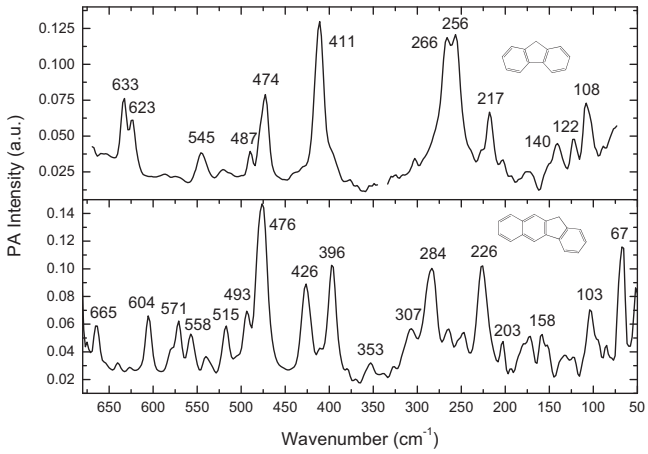

Fig. 2. Low wavenumber PA infrared spectra of fluorene (top panel) and 2,3-benzofluorene (bottom panel). Spurious data near 340 cm^{-1} have been removed from the fluorene spectrum.

used to correct sample spectra for the wavenumber-dependent response of each instrument.

3.3. Mid-infrared spectra

PA mid-infrared spectra were recorded at a resolution of 6 cm^{-1} using the Bruker IFS 88 spectrometer mentioned above. The laser frequency was either 1.6 or 2.2 kHz. An MTEC 200 PA cell was utilized. Nitrogen was used to purge the spectrometer and as a carrier gas. A KBr window sealed the PA cell, and a Ge/KBr beamsplitter was used in the spectrometer. Ten 32-scan spectra were averaged for each sample. Spectra were acquired from about 4000 to 400 cm^{-1}. Data are reported up to 2000 cm^{-1} in the body of this article. Data for the higher wavenumber region are summarized in the Supplementary material. Carbon black powder was used to obtain reference spectra in these experiments.

4. Results and discussion

Raman and PA infrared spectra of the five compounds studied in this work are discussed in the following two sections. The 'low wavenumber' (~700–100 cm^{-1}; commonly referred to as far infrared) and 'fingerprint' (2000–700 cm^{-1}) regions are defined according to infrared spectroscopy convention. For convenience, the Raman and infrared data share the same demarcation limits, and are presented jointly in each section.

4.1. Low wavenumber region (~700–100 cm^{-1})

4.1.1. Fluorene and 2,3-benzofluorene

Raman spectra of fluorene and 2,3-benzofluorene (also known as 11*H*-benzo[*b*]fluorene or isonaphthofluorene) are displayed in Fig. 1, with the corresponding PA infrared spectra appearing in Fig. 2. The predominance of the bands at 280 and 417 cm^{-1} in the Raman spectrum of fluorene (Fig. 1, upper curve) is a particularly noticeable result, as is the rather large number of bands in the PA spectra (Fig. 2). Tables 1 and 2 summarize band positions and relative intensities in the low wavenumber Raman and infrared spectra of both compounds, alongside the corresponding results from the harmonic and anharmonic calculations (including infrared intensities) performed in this work. Symmetry classifications for the fundamental modes are also given in these tables. Predicted frequencies and intensities for all modes, including those at higher wavenumbers, are listed in the Supplementary material.

As discussed previously [2], the reported DFT calculations are not scaled. Consequently, the predicted values in column 3 of each table tend to be a few percent higher than their scaled counterparts (where these exist) in the literature. Scaling provides a correction (adjustment) for anharmonicity, but produces only small changes in the low wavenumber region. The discrepancies between predicted and observed frequencies are generally greater than these minor adjustments and there is no compelling reason to scale the DFT calculations. Treatment of anharmonicity using the variational method described in Section 2.2 is more appropriate. This method, which predicts fundamental, combination and overtone frequencies, as well as intensities, yielded the values reported in columns 4 and 5 of Tables 1 and 2. Several attributions to dimer vibrations are indicated in these tables and infrared- and Raman-active modes are denoted 'd' and 'Rd', respectively. Assignments to combinations and overtones, listed in column 5, provide interpretations of a number of weak features in the spectra. Correlations between the respective fundamental frequencies obtained via the DFT and variational methods (columns 3 and 4) for both compounds were generally straightforward. As predicted intensities were also considered during correlation development, two out-of-sequence pairs of close-lying frequencies in column 5 of Table 2 were identified.

4.1.2. 2-Methylfluorene, 2-ethylfluorene and 1,8-dimethylfluorene

Low wavenumber Raman spectra of three alkyl fluorene derivatives (2-methylfluorene, 2-ethylfluorene and 1,8-dimethylfluorene) are shown in Fig. 3, while the PA infrared spectra are shown in Fig. 4. (Spurious features have been removed from two spectra in Figs. 2 and 4, producing small gaps in the data.) The Raman spectra are presented using greatly different intensity scales, as is mandated by the diverse intensities observed for these three substances in this region. The recorded spectrum for 2-ethylfluorene is from one to two orders of magnitude weaker than those of the two other compounds, probably because of the very small quantity of 2-ethylfluorene available for analysis. By contrast, PA intensities in the infrared spectra of the three alkyl derivatives are not disparate (Fig. 4). The PA spectra for these compounds are not reported below 200 cm^{-1} to avoid artifacts and noise arising in this region. Despite this limitation, the Raman and PA infrared spectra in Figs. 3 and 4 comprise some of the first known low wavenumber data for these compounds.

Tables 3–5 list the wavenumbers and relative intensities of the observed bands for 2-methylfluorene, 2-ethylfluorene and 1,8-dimethylfluorene, respectively. Symmetry classifications are

Table 1
Low wavenumber Raman and PA infrared spectra of fluorene (C_{2v}).

Observed		Predicted[a]			
Raman[b]	Infrared[b]	Symmetry	Harmonic[c]	Anharmonic[d]	Combination[d]
696 vw	697 s	b_1	710 (5.4)	713 (2.9)	
				710 (0.1)	277 + 433
				693 (0.1)	140 + 580
	667 sh			664 (0.6)	248 + 416
	650 vw			654(0.1)	99 + 558
632 vw	633 w	a_1	645 (0.3)	650 (0.5)[e]	
	623 w	b_2	636 (7.7)	645 (8.1)	
	587 vw				
	573 vw	a_2	574 (0.0)	580 (0.0)	
562 vw				571 Rd	
542 m	545 w	b_2	553 (0.1)	558 (0.1)	
				546 (0.1)[f]	140 + 433
	519 w				
482 vw	487 w	b_2	498 (0.3)	498 (0.4)	
471 vw	474 m	b_1	479 (0.8)	488 (2.0)	
427 sh	428 sh	a_2	437 (0.0)	433 (0.0)	
417 s		a_1	419 (0.4)	420 (0.3)	
411 sh	411 s	b_1	421 (6.2)	416 (7.2), 429 Rd	
367 vw				362 (1.2)	140 + 248
	302 w				
280 s		a_2	273 (0.0)	277 (0.0)	
	266 m				
255 vw	256 m	b_1	240 (7.3)	248 (8.0)	
217 m	217 m	a_1	217 (0.2)	211 (0.2), 221 d	
	172 w				
156 vw	151 vw			157 d	
	140 w	a_2	136 (0.0)	140 (0.0)	
	122 w				
	108 m	b_1	98 (0.6)	99 (0.7)	

[a] Infrared intensities (in parentheses) in km/mol.
[b] Estimated uncertainties in band positions are within ±3 cm^{-1}. Relative intensities: vw = very weak, w = weak, m = medium, s = strong, vs = very strong, sh = shoulder.
[c] Unscaled DFT frequencies calculated using B3LYP/6-311+G(d,p) as described elsewhere [3].
[d] Anharmonics B3LYP/6-311 calculation using the P_VMWCl$_2$ algorithm [21,22]. d = infrared-active dimer vibration, Rd = Raman-active dimer vibration.
[e] Eigenvector contains 10% contribution from 416 + 211 cm^{-1} combination.
[f] Eigenvector contains 12% contribution from 416 + 99 cm^{-1} combination.

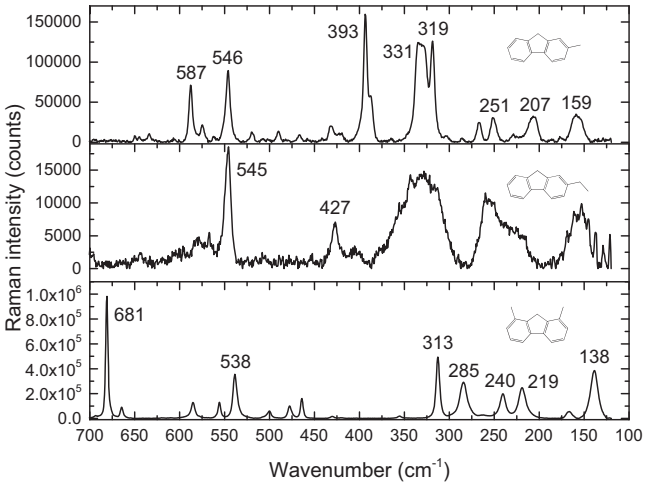

Fig. 3. Low wavenumber Raman spectra of 2-methylfluorene (top panel), 2-ethylfluorene (middle panel) and 1,8-dimethylfluorene (bottom panel).

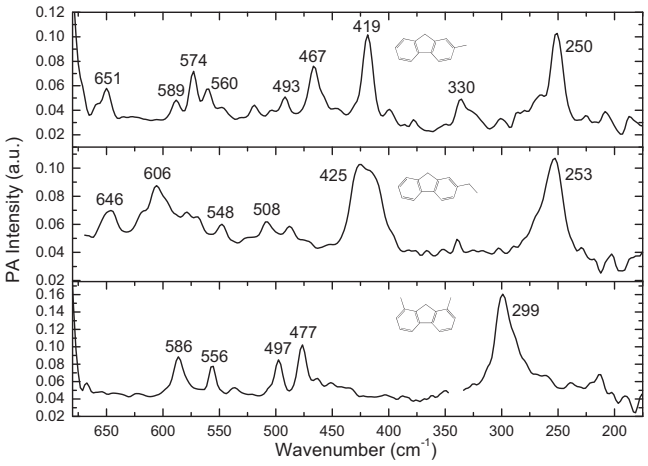

Fig. 4. Low wavenumber PA infrared spectra of 2-methylfluorene (top panel), 2-ethylfluorene (middle panel) and 1,8-dimethylfluorene (bottom panel). Spurious data near 340 cm^{-1} have been removed from the 1,8-dimethylfluorene spectrum.

included for 1,8-dimethylfluorene in column 3 of Table 5. The lower symmetries of 2-methylfluorene and 2-ethylfluorene (C_1) obviate the need for comparable classifications in Tables 3 and 4. Predicted harmonic and anharmonic frequencies are given in each table according to the convention established for Tables 1 and 2. The anharmonic calculations yielded several dimer vibrations, as well as combinations and overtones (columns 4 and 5). Both intensities and wavenumbers obtained in the harmonic and variational calculations were taken into account as the individual bands in the Raman and infrared spectra were correlated with the predictions. As is the case for fluorene and 2,3-benzofluorene, the low wavenumber Raman and PA infrared spectra of the alkyl-substituted fluorenes contain much detail; sufficient information for the identification and characterization of these compounds.

The lowest calculated fundamental frequencies for 2-methylfluorene in Table 3 (harmonic, 24 cm^{-1}; anharmonic, 20 cm^{-1}) lie beyond the low wavenumber cutoff of the mylar beamsplitters used for the far-infrared measurements. Attempts

Table 2
Low wavenumber Raman and PA infrared spectra of 2,3-benzofluorene (C_s).

Observed		Predicted[a]			
Raman[b]	Infrared[b]	Symmetry	Harmonic[c]	Anharmonic[d]	Combination or overtone[d]
700 w	700 sh	a′	713 (2.1)	719 (1.4)	
680 vw					
	665 w	a″	677 (0.7)	683 (1.5)	
	640 vw	a′	644 (0.1)	654 (0.1)	
627 vw	626 vw	a′	617 (2.4)	627 (0.7)	
605 vw	604 w	a′	582 (8.6)	589 (7.2)	
569 w	571 w	a″	564 (0.3)	573 (0.3)	
	558 w	a′	549 (1.0)	553 (0.7)	
541 m	540 vw				62 + 498
	515 w	a″	501 (0.1)	510 (0.1)	
	493 m	a′	490 (0.4)	498 (0.2)[e]	
479 m	476 s	a″	483 (16.7)	487 (16.4)	
425 w	426 m	a″	435 (1.4)	437 (2.0)	
				427 (0.2)	2 × 213
395 m	396 m	a″	405 (3.1)	408 (3.2)[f]	
355 s	353 w	a′	357 (0.1)	359 (0.1)	
314 sh		a″	312 (0.2)	312 (0.1)	
308 m	307 w	a′	312 (0.7)	315 (0.6)	
289 w	284 m	a″	272 (2.9)	281 (3.2)	
	265 w				
	248 w			255 (0.2)	94 + 213
223 m	226 m			239 (0.1)	94 + 156
	203 w	a″	206 (2.3)	213 (2.0)	
169 s	172 w			161 (0.1)	62 + 94
158 s	158 w	a′	156 (0.1)	156 (0.5)	
	152 sh	a″	155 (0.6)	158 (0.1)	
144 vw					
138 w	133 w			139 d	
129 w	122 w			123 (0.1)	2 × 62
	103 m	a″	95 (0.2)	94 (0.1)	
	67 m	a″	62 (0.5)	62 (0.5)	

[a] Infrared intensities (in parentheses) in km/mol.
[b] Estimated uncertainties in band positions are within ±3 cm^{-1}. Relative intensities: vw = very weak, w = weak, m = medium, s = strong, vs = very strong, sh = shoulder.
[c] Unscaled DFT frequencies calculated using B3LYP/6-311+G(d,p) as described elsewhere [3].
[d] Anharmonics B3LYP/6-311 calculation using the P_VMWCl$_2$ algorithm [21,22]. d = infrared-active dimer vibration.
[e] Eigenvector contains 9% contribution from 281 + 213 cm^{-1} combination.
[f] Eigenvector contains 5% contribution from 804 cm^{-1} mode.

are currently underway to study this region in separate experiments at the Canadian Light Source. This work entails the use of coherent synchrotron radiation [23] in place of a conventional optical source for PA infrared spectroscopy. The currently accessible region in this experiment [24], which employs a Bruker IFS 125HR spectrometer and a different beamsplitter, extends from about 5 to 25 cm^{-1}. Initial experiments have produced inconclusive results but this investigation is ongoing.

4.2. Fingerprint region (2000–700 cm^{-1})

4.2.1. Fluorene and 2,3-benzofluorene

The 2000–700 cm^{-1} regions of the observed Raman and PA spectra for fluorene and 2,3-benzofluorene are shown in Figs. 5 and 6, respectively. Several noteworthy aspects of these spectra are immediately apparent. These include (a) very good band definition and contrast in the Raman spectra; (b) significantly greater bandwidths and the absence of void regions in the PA infrared spectra; and (c) prominent overtone and combination bands above 1640 cm^{-1} in both PA spectra. Comparison of the upper and lower panels in Fig. 5 also reveals a few near-coincidences of Raman bands for the two compounds, consistent with their structural similarity.

Band positions and relative intensities in Figs. 5 and 6 for the experimental measurements and the calculations are summarized in Table 6 (fluorene) and 7 (2,3-benzofluorene). The predicted wavenumbers appear in columns 3 and 4 of these tables, regardless of the presence or absence of corresponding bands in the measured spectra and they were interpreted in the same manner as the low wavenumber calculations. Most of the combinations and overtones

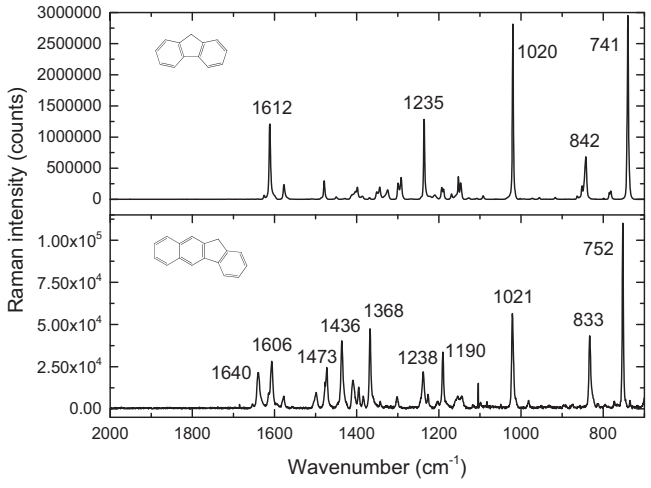

Fig. 5. Fingerprint region Raman spectra of fluorene (top panel) and 2,3-benzofluorene (bottom panel).

at higher wavenumbers in the infrared spectra are predicted in the variational calculations. Minor unassigned bands in both the Raman and PA spectra presumably have analogous origins.

The assignments of the combination and overtone bands above 1640 cm^{-1} in the PA infrared spectra deserve further comment. Tables 6 and 7 show that these attributions involve medium- or strong-intensity bands between about 1100 and 700 cm^{-1} for the most part. The DFT and anharmonic calculations confirm

Table 3
Low wavenumber Raman and PA infrared spectra of 2-methylfluorene (C_1).

Observed		Predicted[a]		
Raman[b]	Infrared[b]	Harmonic[c]	Anharmonic[d]	Combination or overtone[d]
	675 m	658 (1.4)	660 (0.5)	
650 vw	651 m			69 + 591
644 vw				
634 vw				
	618 vw			
607 vw				
587 w	589 sh			
575 vw	574 m	586 (2.4)	591 (1.7)	
562 vw	560 vw	582 (2.1)	589 (2.0)	
546 m	546 vw	555 (0.9)	560 (0.5)	
520 vw	518 vw	512 (0.4)	516 (0.3)	
490 vw	493 vw	499 (0.7)	506 (0.3)[e]	2 × 250
467 vw	467 m			
432 vw		436 (0.2)	437 (0.1)	
421 vw	419 m	426 (9.0)	434 (6.1)[f]	
393 m	395 vw	397 (0.2)	398 (0.2)	
387 sh				
365 vw				
331 m	330 w	327 (0.9)	331 (0.2)	
319 m		319 (0.1)	319 (0.1)	
304 vw	303 vw			
286 vw	285 sh			
267 w			270 Rd	
251 w	250 m	240 (6.8)	250 (3.0)	
229 vw	226 vw			
207 w	206 vw	194 (0.3)	198 (0.4)	
177 vw		185 (0.4)	183 (0.1)	
159 w			142 (0.1)	20 +132
		134 (0.1)	132 (0.1)	
		72 (0.6)	69 (0.3)	
		24 (0.3)	20 (0.2)	

[a] Infrared intensities (in parentheses) in km/mol.
[b] Estimated uncertainties in band positions are within ±3 cm^{-1}. Relative intensities: vw = very weak, w = weak, m = medium, s = strong, vs = very strong, sh = shoulder.
[c] Unscaled DFT frequencies calculated using B3LYP/6-311+G(d,p) as described elsewhere [3].
[d] Anharmonics B3LYP/6-311 calculation using the P_VMWCl$_2$ algorithm [21,22]. Rd = Raman-active dimer vibration.
[e] Eigenvector contains 7% contribution from 3 × 250 cm^{-1} overtone.
[f] Eigenvector contains 6% contribution from 250 + 132 cm^{-1} combination.

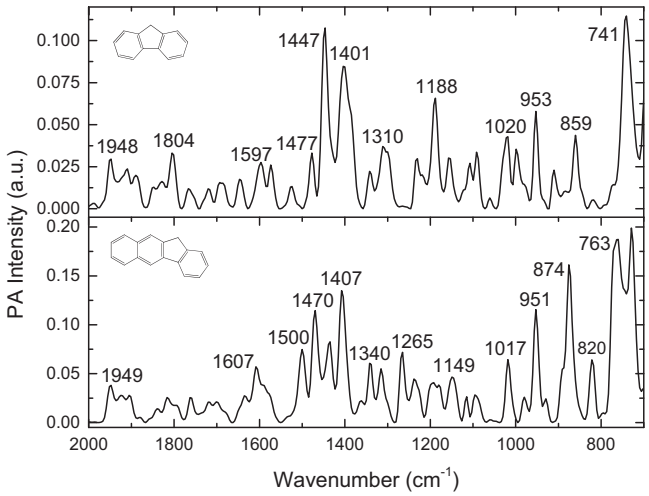

Fig. 6. Fingerprint region PA infrared spectra of fluorene (top panel) and 2,3-benzofluorene (bottom panel).

that many of these bands arise from a_2 and b_1 (fluorene; C_{2v} symmetry) or a″ (2,3-benzofluorene; C_s symmetry) modes. The vibrations implicated below ∼1000 cm^{-1} generally entail out-of-plane displacement of carbon–carbon and carbon–hydrogen groups. Combination bands in the 2000–1640 cm^{-1} region involving non-planar CH vibrations have been reported previously [2,5–7]. Hence this aspect of the present work is consistent with previously published literature.

Spectral data for fluorene also provide points of contact with the analytical [25–28] and applied [29–32] literatures. Infrared [25–28] and Raman [26–28] spectra for fluorene are available. The single crystal study of Bree and Zwarich [26] is particularly informative. UV-excited Raman spectra of fluorene were reported by Asher and coworkers as part of their studies of coal liquids [29,30]. Similarly, Chua and Stair discussed UV Raman spectra of fluorene and several polyaromatic compounds in an investigation of methanol-to-hydrocarbons conversion [31]. Raman spectra of fluorene adsorbed on TiO_2 were obtained as part of a photocatalytic study by Cordeiro and Corio [32]. The band locations in these publications generally agree with their counterparts in columns 1 and 2 of Tables 1 and 6, although the relative intensities differ in some cases due to the diverse experimental conditions employed in these works. A recent publication on gas phase infrared spectra of fluorene, 1-methylfluorene and 1,8-dimethylfluorene [33] reports both harmonic and anharmonic calculated frequencies, the former agreeing with the present results to within ±2 cm^{-1} in most cases. The anharmonic frequencies in their work were fitted to gas phase data, and thus show much poorer agreement with the values computed in this work.

For 2,3-benzofluorene an experimental infrared and DFT investigation of neutral and cationic 2,3-benzofluorene [34] is available for comparison. This article reports calculated frequencies for most, but not all, infrared-active fundamentals. These frequencies, which are scaled, are generally similar to the respective anharmonic frequencies reported in column 5 of Table 7.

Table 4
Low wavenumber Raman and PA infrared spectra of 2-ethylfluorene (C_1).

Observed		Predicted[a]		
Raman[b]	Infrared[b]	Harmonic[c]	Anharmonic[d]	Combination or overtone[d]
	646 m	657 (1.6)	664 (1.6)	
	606 m	619 (4.4)	626 (4.0)	
580 vw	578 vw			
567 vw	569 sh	578 (1.7)	575 (1.1)[e]	
545 w	548 w	554 (0.7)	561 (0.5)	
	525 sh	517 (1.0)	529 (0.4)	
		512 (0.6)	519 (0.6)	
505 vw	508 w		503 (0.1)	247 + 259
	487 w		493 (0.5)[f]	2 × 247
454 vw			460 Rd	
		437 (0.6)	441 (1.2)	
427 w	425 s	434 (6.2)	443 (5.8)	
	416 sh			
404 vw		410 (1.8)	409 (1.2)	
343 vw	340 vw	367 (0.1)	374 (0.1)	
330 vw		327 (0.2)	330 (0.2)	
		258 (0.2)	259 (0.2)	
255 vw	253 s	240 (6.7)	247 (7.1)	
226 vw		229 (0.1)	215 (0.1)	
169 vw	172 w	174 (0.2)	175 (0.2)	
152 vw		148 (0.1)	151 (0.1)	
145 vw			148 Rd	
138 vw				
129 vw		129 (0.1)	130 (0.1)	
		58 (0.4)	57 (0.3)	
		34 (0.1)	32 (0.1)	

[a] Infrared intensities (in parentheses) in km/mol.
[b] Estimated uncertainties in band positions are within ±3 cm^{-1}. Relative intensities: vw = very weak, w = weak, m = medium, s = strong, vs = very strong, sh = shoulder.
[c] Unscaled DFT frequencies calculated using B3LYP/6-311+G(d,p) as described elsewhere [3].
[d] Anharmonics B3LYP/6-311 calculation using the P_VMWCl$_2$ algorithm [21,22]. Rd = Raman-active dimer vibration.
[e] Eigenvector contains 8% contribution from 330 + 247 cm^{-1} combination.
[f] Eigenvector contains 6% contribution from 3 × 247 cm^{-1} overtone and 5% contribution from 247 cm^{-1} mode.

The 1075–990 cm^{-1} region of the PA infrared spectra of fluorene and 2,3-benzofluorene was also examined in our laboratory using a quantum cascade laser (QCL) as the infrared radiation source. Laser-based PA infrared spectra typically display much narrower bands than those in FT-IR spectra [35,36], often facilitating observation of shoulders and detection of weak bands. This brief study suggested probable new features at approximately 994, 996 and 1032 cm^{-1} for fluorene, the two lower frequency bands possibly corresponding to similar calculated frequencies in columns 4 and 5 of Table 6. The 2,3-benzofluorene spectrum displayed bands at 1017 and 1021 cm^{-1}, the latter feature being revealed due to reduced band widths. Hence additional useful information was acquired in the QCL experiment, despite the narrow range of the measurements.

4.2.2. 2-Methylfluorene, 2-ethylfluorene and 1,8-dimethylfluorene

The fingerprint regions of the Raman and PA spectra obtained for the alkyl derivatives of fluorene are shown in Figs. 7 and 8, respectively. The Raman spectra display a number of well-defined bands, with intensities ranging over multiple orders of magnitude. By contrast the PA infrared spectra exhibit characteristically wider bands, which occur within a much smaller dynamic range. As noted in the previous section, the PA spectra include an appreciable number of bands throughout the entire 2000–700 cm^{-1} region, while the Raman spectra do not contain significant features above approximately 1750 cm^{-1}.

Experimental and computed wavenumbers and intensities for the alkylated fluorenes are reported in Tables 8–10. No previously published calculations are known for these compounds. Correlations between the observed and calculated bands were developed using both position and intensity information, the majority of these assignments being relatively straightforward. Nevertheless, the existence of large numbers of fundamentals for the substituted compounds inevitably leads to a few ambiguities. Additionally, there is a tendency for neighboring vibrations to occur very close to one another in particular regions (e.g., ~1500 and ~1600 cm^{-1}). More bands may be calculated than observed in some cases, implying that it is not always feasible to make definitive assignments. Again, all predicted frequencies appear in the tables, irrespective of the number of bands actually observed in the spectra.

These tables also present a number of assignments to combinations and overtones of infrared-active vibrations between ~1500 and 700 cm^{-1}. Calculated anharmonic frequencies were used for these attributions, often leading to predicted frequencies slightly

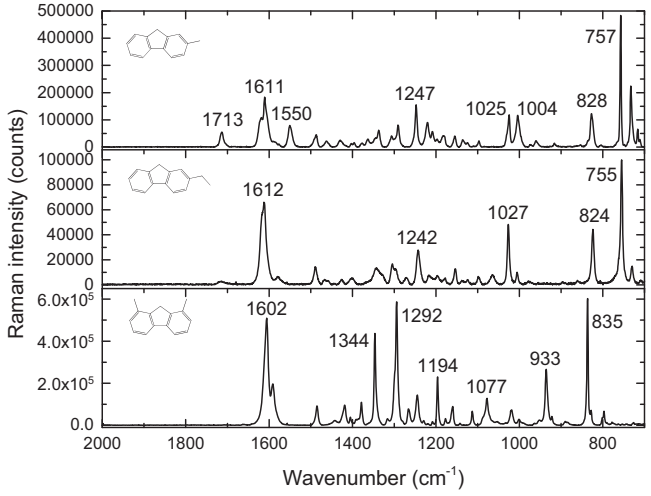

Fig. 7. Fingerprint region Raman spectra of 2-methylfluorene (top panel), 2-ethylfluorene (middle panel) and 1,8-dimethylfluorene (bottom panel).

Table 5
Low wavenumber Raman and PA infrared spectra of 1,8-dimethylfluorene (C_{2v}).

Observed		Predicted[a]			
Raman[b]	Infrared[b]	Symmetry	Harmonic[c]	Anharmonic[d]	Combination[d]
694 vw	693 m	b_1	709 (8.5)	699 (4.2)	
681 vs		a_1	692 (0.1)	692 (0.2)	
664 w	668 vw				
	645 vw			650 (0.1)	113 + 543
	622 vw			616 (0.2)	113 + 506
		a_2	599 (0.0)	589 (0.0)	
585 w	586 m	b_2	594 (4.3)	598 (3.6)	
	556 m	b_2	566 (3.0)	571 (3.3)	
538 m	536 w	a_1	544 (0.6)	543 (0.4)	
		b_1	511 (1.0)	513 (0.9)	
500 m	497 m	a_2	510 (0.0)	506 (0.0)	
478 w	477 m	b_2	485 (0.2)	481 (1.1)	
464 w	464 vw	b_1	481 (0.3)	476 (0.1)[e]	
		a_1	468 (0.4)	460 (0.2)[f]	
	451 vw			460 (0.1)	147 + 316
430 vw				431 (0.2)	147 + 286
	403 vw			397 (0.3)	113 + 286
	387 vw				
356 vw					
313 m		a_1	312 (0.1)	316 (0.1)	
	299 s	b_2	278 (0.1)	276 (0.1)	
285 m		a_2	276 (0.0)	286 (0.0)	
264 vw	261 sh	b_1	259 (11.3)	267 (12.0)	
240 m	238 w	a_2	232 (0.0)	236 (0.0)	
219 m	213 w	b_1	199 (0.1)	202 (0.1)	
166 w	166 vw				
138 m	138 w	a_1	159 (0.1)	147 (0.1)	
		a_2	115 (0.0)	115 (0.0)	
	121 m	b_1	111 (0.6)	113 (0.6)	
		b_1	90 (0.7)	90 (0.2)	
		a_2	83 (0.0)	83 (0.0)	

[a] Infrared intensities (in parentheses) in km/mol.
[b] Estimated uncertainties in band positions are within ±3 cm^{-1}. Relative intensities: vw = very weak, w = weak, m = medium, s = strong, vs = very strong, sh = shoulder.
[c] Unscaled DFT frequencies calculated using B3LYP/6-311+G(d,p) as described elsewhere [3].
[d] Anharmonics B3LYP/6-311 calculation using the P_VMWCl$_2$ algorithm [21,22].
[e] A Raman-active dimer vibration was also calculated at 476 cm^{-1}.
[f] Eigenvector contains 11% contribution from 3 × 147 cm^{-1} overtone.

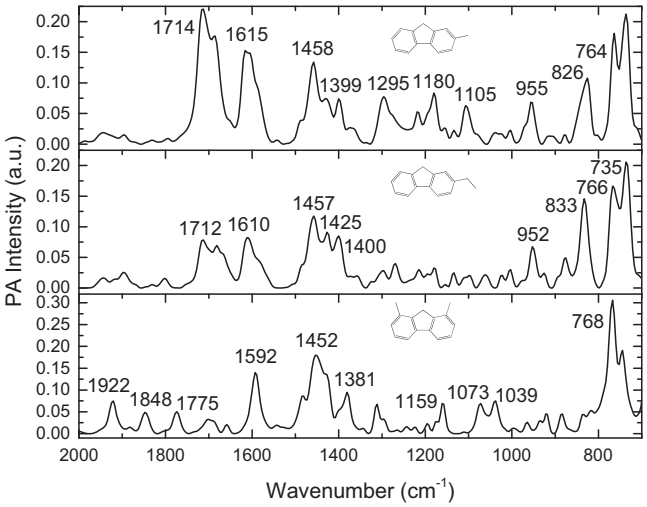

Fig. 8. Fingerprint region PA infrared spectra of 2-methylfluorene (top panel), 2-ethylfluorene (middle panel) and 1,8-dimethylfluorene (bottom panel).

higher than the corresponding experimental values. While most of the listed combinations occur above ~1650 cm^{-1}, a few of the weak features at lower wavenumbers undoubtedly have similar origins. It is also interesting to note that vibrations above 1200 cm^{-1} participate in several combinations for the alkyl derivatives, in contrast with those in Tables 6 and 7. It is reasonable to suggest that the alkyl substituents may play a role in the appearance of these bands.

5. Summary

Raman and PA infrared spectra of fluorene, 2,3-benzofluorene, 2-methylfluorene, 2-ethylfluorene and 1,8-dimethylfluorene were acquired and compared with both harmonic (DFT) and anharmonic (variational) calculations in this work. Some of the features observed experimentally were identified for the first time. These include low wavenumber bands for all fluorene derivatives and combination and overtone bands in the low wavenumber and fingerprint regions of the PA infrared spectra. Where available, the measurements in the present work agree with the literature to within applicable experimental errors.

Similarities between the Raman spectra of fluorene and 2,3-benzofluorene were noted in Section 4.2.1. Further examination of the Raman and infrared spectra acquired in this work reveals several regions which contain bands representative of the fluorene family. Characteristic "marker" Raman bands of fluorene (Tables 1 and 6) occur at 417, 542, 741, 842, 1235 and 1612 cm^{-1}; analogous features can be identified for the derivatives (Tables 2–5 and 7–10). The relevant normal modes of the fluorene moiety are illustrated in Table S7 (Supplementary material), which also summarizes the corresponding frequencies in the four derivatives. Similarly, the PA infrared spectra in Figs. 2, 4, 6 and 8 generally exhibit bands near ~470, 750, 1500–1400, and 1575 cm^{-1}. Hence observation of bands in these regions could be taken as confirmation of fluorene-like structures within larger aggregates such as asphaltenes or mixtures of polyaromatic hydrocarbons.

Combination and overtone bands appear throughout the far- and mid-infrared regions of the PA infrared spectra. These

Table 6
Raman and PA infrared spectra of fluorene (C_{2v}), 2000–700 cm^{-1}.

Observed		Predicted[a]			
Raman[b]	Infrared[b]	Symmetry	Harmonic[c]	Anharmonic[d]	Combination or overtone[d]
	1988 vw			1986(0.1)	2 × 995
	1948 m			1964(0.3)[e]	2 × 983
	1909 w			1906(0.1)	2 × 955
	1891 w			1901(0.1)	713 + 1189
	1846 vw			1850(0.3)	752 + 1110
	1830 w			1835(0.3)	853 + 983
	1804 m			1805(0.2)[f]	870 + 936
				1760(0.1)	752 + 1015
	1717 w			1739(0.2)	2 × 870
	1690 w			1695(0.1)	752 + 955
	1645 w			1664(0.1)	713 + 955
1625 w		b_2	1647(4.0)	1610(2.2)[g]	
1612 s	1597 m	a_1	1646(0.1)	1607(0.0)	
1577 m	1573 m	b_2	1621(0.5)	1580(1.5)	
		a_1	1616(1.3)	1601(1.4)	
	1525 w				
		b_2	1508(7.0)	1492(8.1)	
1508 vw		a_1	1507(0.0)	1488(0.5)	
		a_1	1477(8.9)	1482(0.2)	
1479 m	1477 m	b_2	1483(19.0)	1467(20.0)	
1450 vw	1447 vs	a_1	1451(12.2)	1445(20.2)	
1429 vw					
1412 sh					
1403 sh	1401 s			1402(1.5)	416 + 983
1399 w					
1386 vw	1384 sh				
1369 vw					
1351 sh		a_1	1374(0.3)	1370(0.0)	
1344 w	1341 m	b_2	1345(7.1)	1349(8.4)	
1325 w		b_2	1329(2.5)	1328(0.8)	
1300 w	1310 m	a_1	1320(0.4)	1314(4.1)	
1292 m	1300 sh				
1268 vw		a_1	1252(3.0)	1238(4.0)	
1235 vs	1231 w	b_2	1221(3.9)	1208(0.6)	
1221 vw	1219 vw				
1210 vw		a_1	1207(2.9)	1201(0.9)	
1193 w	1188 m	b_2	1192(3.0)	1194(3.1)	
1188 w		a_1	1180(0.1)	1189(0.1)	
1169 vw		b_2	1176(0.2)	1181(0.1)	
1153 m	1155 m	a_2	1162(0.0)	1156(0.2)	
1146 w					
1127 vw	1122 sh				
1115 vw					
1107 vw	1108 m	b_2	1130(0.1)	1119(0.1)	
1092 vw	1091 m	a_1	1117(3.3)	1110(3.0)	
	1061 vw	b_2	1051(5.8)	1047(2.4)	
1020 vs	1020 m	a_1	1045(0.9)	1029(0.7)	
1002 vw					
993 vw	997 m	b_2	1023(4.6)	1015(5.3)	
		b_1	994(0.1)	995(0.2)	
973 vw	979 sh	a_2	993(0.0)	992(0.0)	
955 vw	953 m	b_1	976(4.2)	983(4.7)	
		a_2	956(0.0)	955(0.3)	
917 vw	910 vw	b_1	933(0.1)	936(0.1)	
	881 vw	a_2	880(0.0)	880(0.1)	
864 vw	859 m	b_1	871(0.6)	870(1.2)	
852 w					
842 m		a_1	853(0.1)	853(0.2)	
	820 vw	b_2	813(0.4)	807(0.6)	
786 w	792 vw	a_2	792(0.0)	799(0.1)	
781 w	775 sh				
741 vs		a_1	755(0.1)	743(0.0)	
	741 vs	b_1	754(134.8)	752(132.1)	
		a_2	738(0.0)	736(0.0)	
		b_1	710(5.4)	713(2.9)	

[a] Infrared intensities (in parentheses) in km/mol.
[b] Estimated uncertainties in band positions are within ±3 cm^{-1}. Relative intensities: vw = very weak, w = weak, m = medium, s = strong, vs = very strong, sh = shoulder.
[c] Unscaled DFT frequencies calculated using B3LYP/6-311+G(d,p) as described elsewhere [3].
[d] Anharmonics B3LYP/6-311 calculation using the P_VMWCl$_2$ algorithm [21,22].
[e] Eigenvector contains 6% contribution from 3 × 983 cm^{-1} overtone.
[f] Eigenvector contains 5% contribution from 2 × 870 cm^{-1} overtone.
[g] Eigenvector contains 7% contribution from 807 + 743 cm^{-1} combination.

Table 7
Raman and PA infrared spectra of 2,3-benzofluorene (C_s), 2000–700 cm^{-1}.

Observed		Predicted[a]			
Raman[b]	Infrared[b]	Symmetry	Harmonic[c]	Anharmonic[d]	Combination or overtone[d]
	1949 w				
	1924 w			1891 (0.3)[e]	892 + 1027
	1905 w			1898 (0.1)	2 × 950
	1880 vw				
	1840 vw			1825 (0.3)	892 + 950
	1815 w			1831 (0.7)	804 + 1027
	1792 sh			1783 (0.1)	760 + 1027
	1761 w				
	1719 w			1738 (0.1)	760 + 950
	1700 w			1714 (0.1), 1696 (0.1)	804 + 914, 804 + 892
1640 m	1635 w	a′	1673 (2.7)	1642 (1.0)[f]	
		a′	1649 (1.5)	1616 (2.2)	
1606 m	1607 m	a′	1645 (1.0)	1614 (0.7)	
		a′	1620 (1.5)	1608 (0.4)	
1577 w		a′	1613 (1.0)	1577 (0.3)	
1499 m	1500 m	a′	1536 (12.1)	1517 (11.1)	
1473 m	1470 m	a′	1503 (3.9)	1482 (0.9)	
		a′	1500 (6.8)	1489 (0.2)	
		a′	1479 (2.9)	1477 (0.1)	
		a′	1467 (14.0)	1466 (5.1)	
1436 s	1436 m	a′	1455 (14.3)	1444 (18.8)	
1409 m	1407 m	a′	1425 (0.2)	1410 (1.9)	
1395 w		a′	1390 (0.8)	1386 (0.2)	
1384 w					
1368 s	1363 vw	a′	1368 (2.6)	1361 (1.0)	
1342 vw	1340 m	a′	1351 (8.6)	1334 (4.9)	
	1315 m	a′	1326 (0.1)	1320 (0.0)	
1302 vw					
	1265 m	a′	1283 (5.1)	1289 (5.6)	
		a′	1261 (0.9)	1256 (0.1)	
1238 m	1236 w	a′	1250 (1.7)	1243 (1.5)	
1226 w		a′	1224 (0.6)	1225 (0.1)[g]	
1204 vw		a′	1213 (6.6)	1206 (0.2)	
1190 m	1194 w	a′	1197 (1.6)	1187 (2.6)	
	1179 sh	a′	1179 (0.3)	1176 (0.5)	
1154 w	1149 m	a′	1174 (3.6)	1170 (3.5)	
		a′	1169 (2.7)	1160 (0.1)	
1144 w		a″	1165 (0.1)	1142 (0.0)	
1117 vw	1116 w	a′	1136 (2.6)	1125 (1.3)	
1099 vw	1094 w	a′	1116 (0.9)	1110 (0.9)	
	1058 vw	a′	1046 (5.5)	1044 (0.1)	
1021 s	1017 m	a′	1041 (4.2)	1027 (3.8)	
		a′	998 (0.9)	997 (0.2)	
		a″	994 (0.1)	990 (0.1)	
		a″	993 (0.1)	990 (0.1)	
981 w	978 w	a″	976 (8.2)	984 (1.5)	
		a″	969 (0.5)	974 (0.9)	
951 vw	951 m	a″	946 (0.8)	950 (0.2)	
931 vw	928 w	a′	909 (0.4)	914 (0.3)	
896 vw		a″	903 (2.4)	914 (0.5)	
876 vw	874 s	a″	888 (27.9)	892 (27.7)	
		a″	876 (0.3)	870 (0.1)	
		a″	857 (0.1)	852 (0.1)	
833 s		a′	842 (0.1)	842 (0.3)	
814 vw	820 m	a″	782 (49.6)	804 (12.4)	
796 vw		a′	803 (0.1)	797 (0.1)	
773 w		a″	772 (14.2)	776 (3.8)	
	763 s	a′	766 (0.1)	759 (0.1)	
752 vs		a″	755 (12.9)	760 (14.2)	
734 w	728 s	a″	736 (44.0)	741 (44.8)	
700 w	700 sh	a′	713 (2.1)	719 (1.4)	

[a] Infrared intensities (in parentheses) in km/mol.
[b] Estimated uncertainties in band positions are within ±3 cm^{-1}. Relative intensities: vw = very weak, w = weak, m = medium, s = strong, vs = very strong, sh = shoulder.
[c] Unscaled DFT frequencies calculated using B3LYP/6-311+G(d,p) as described elsewhere [3].
[d] Anharmonics B3LYP/6-311 calculation using the P_VMWCl$_2$ algorithm [21,22].
[e] Eigenvector contains 5% contribution from 852 + 842 cm^{-1} combination.
[f] Eigenvector contains 10% contribution from 2 × 804 cm^{-1} overtone and 5% contribution from 2 × 792 cm^{-1} overtone.
[g] A Raman-active dimer vibration was also calculated at 1231 cm^{-1}.

Table 8
Raman and PA infrared spectra of 2-methylfluorene (C_1), 2000–700 cm^{-1}.

Observed		Predicted[a]		
Raman[b]	Infrared[b]	Harmonic[c]	Anharmonic[d]	Combination or overtone[d]
	1945 w		1964(0.8)	756+1216
	1896 w			
	1831 vw		1849(0.1)[e]	756+1109
	1795 vw		1802(0.1)	591+1216
1713 m	1714 vs	1654(3.9)	1610(4.2)	
	1686 sh	1646(6.0)	1600(3.5)	
	1652 vw		1658(1.1)[f]	2 × 830
1619 sh	1615 s	1620(0.4)	1584(3.2)	
1611 m	1605 sh	1614(2.2)	1572(0.7)	
1587 sh				
1577 vw				
1550 m	1543 vw			
		1517(7.2)	1504(7.0)	
		1504(8.0)	1489(10.8)[g]	
1487 w	1487 sh	1491(21.2)	1480(15.2)	
		1489(7.1)	1473(15.0)	
1462 w	1458 s	1484(14.2)	1469(12.8)	
1430 w	1429 sh	1452(4.0)	1450(2.0)	
1403 vw		1449(2.5)	1436(5.6)	
			1416(0.2)	434+987
1395 vw	1399 m	1413(0.1)	1404(0.0)	
1378 vw	1375 sh		1401(0.3)	250+1153
1364 vw	1366 sh	1371(0.4)	1360(0.6)	
1345 sh				
1337 w	1336 vw	1336(12.7)	1328(3.0)	
1306 w		1327(1.1)	1315(4.6)	
1291 m	1295 m	1316(0.9)	1314(0.5)	
1247 m	1247 vw	1267(2.3)	1246(2.0)	
		1236(1.9)	1235(1.1)	
1220 m	1218 m	1221(3.0)	1216(1.8)	
1208 w				
1197 vw	1195 sh	1198(3.4)	1195(3.0)	
1182 w	1180 m	1179(0.3)	1183(0.1)	
		1162(0.1)	1158(0.0)	
1154 w	1156 vw	1157(2.7)	1153(1.6)	
	1105 m	1120(1.9)	1109(1.8)	
1097 w		1059(11.4)	1081(5.0)	
	1039 w	1048(4.8)	1043(6.6)	
1025 m	1026 sh	1024(3.1)	1030(0.6)	
1004 m	1003 w	1015(0.3)	1019(0.1)	
		992(0.1)	987(0.0)	
974 vw	972 sh	974(3.6)	987(2.2)	
960 w	955 m	961(0.3)	964(0.1)	
		941(0.3)	936(0.2)	
916 vw	916 w	927(0.8)	919(0.8)	
	878 w	889(1.9)	910(1.1)	
853 vw	820 m	874(0.1)	877(0.0)	
		837(1.2)	831(0.4)	
828 m	826 s	833(18.2)	830(15.0)	
804 vw	804 vw			
	764 vs	776(45.3)	786(44.5)	
757 vs		771(1.3)	763(0.2)	
733 m	736 vs	743(39.6)	756(39.0)	
716 w		722(1.1)	723(0.9)	
710 vw		711(0.1)	721(0.1)	

[a] Infrared intensities (in parentheses) in km/mol.
[b] Estimated uncertainties in band positions are within ±3 cm^{-1}. Relative intensities: vw = very weak, w = weak, m = medium, s = strong, vs = very strong, sh = shoulder.
[c] Unscaled DFT frequencies calculated using B3LYP/6-311+G(d,p) as described elsewhere [3].
[d] Anharmonics B3LYP/6-311 calculation using the P_VMWCl$_2$ algorithm [21,22].
[e] Eigenvector contains 5% contribution from 1019 + 830 cm^{-1} combination.
[f] Eigenvector contains 8% contribution from 2 × 831 cm^{-1} overtone and 5% contribution from 831 + 830 cm^{-1} combination.
[g] Eigenvector contains 7% contribution from 763 + 756 cm^{-1} combination.

features are most noticeable between about 2700 and 1640 cm^{-1}, since no fundamental vibrations occur in this interval for the compounds studied in this work. The occurrence of these features in PA spectra of condensed-ring hydrocarbons appears to be a general phenomenon. This contention is supported by separate PA measurements made using a quantum cascade laser [36].

The computed spectra and the measured spectra agree with one another with respect to the values of the wavenumbers. Relative peak intensities show poorer agreement due to several factors. These include partial saturation in the PA spectra, which tends to limit the intensities of strong bands while enhancing relative intensities of weaker features. Saturation also tends to increase bandwidths. Moreover, the experimental Raman and infrared spectra are affected by solid-state interactions which are not explicitly taken into consideration in the DFT calculations. Our choice of basis set for these calculations could be another relevant factor. As a

Table 9
Raman and PA infrared spectra of 2-ethylfluorene (C_1), 2000–700 cm^{-1}.

Observed		Predicted[a]		
Raman[b]	Infrared[b]	Harmonic[c]	Anharmonic[d]	Combination or overtone[d]
	1943 vw		1967 (0.1)	891 + 1077
	1917 sh		1900 (0.1)	744 + 1160
	1895 w		1894 (0.1)	2 × 949
	1830 vw		1831 (0.8)	744 + 1077
	1799 w			
1715 vw	1712 m		1704 (0.9)	2 × 853
	1683 w			
1612 vs	1610 m	1652 (1.9)	1626 (2.5)	
1579 w		1646 (6.0)	1614 (3.6)	
		1619 (0.6)	1607 (0.3)	
	1540 sh	1612 (1.0)	1579 (0.9)	
		1517 (7.5)	1510 (0.2)[e]	
		1508 (3.2)	1506 (0.3)	
		1498 (13.1)	1495 (0.5)	
1489 w		1497 (10.0)	1480 (1.4)	
1468 vw		1491 (7.4)	1489 (6.4)	
1459 vw	1457 m	1486 (9.9)	1477 (14.0)	
1443 vw		1457 (7.8)	1440 (10.9)	
1426 w	1425 m	1451 (9.8)	1428 (3.5)	
1402 w	1400 m	1409 (3.4)	1400 (3.2)	
		1374 (0.1)	1368 (0.1)	
	1359 vw	1352 (2.8)	1349 (2.8)	
		1343 (15.3)	1339 (2.3)	
1343 m		1327 (0.5)	1320 (1.1)	
1305 m		1321 (1.2)	1314 (1.7)	
1297 sh	1299 w			
		1271 (1.0)	1270 (0.4)	
1271 w	1269 w	1264 (1.6)	1265 (0.6)	
1242 m		1234 (2.2)	1249 (0.3)	
1217 vw	1215 w	1220 (3.0)	1214 (2.0)	
1196 vw	1194 vw	1198 (3.7)	1197 (3.0)	
1178 vw	1179 w	1179 (0.2)	1194 (0.1)	
		1161 (0.1)	1152 (0.0)	
1154 w	1152 vw	1158 (3.6)	1160 (4.0)	
1137 vw	1137 w	1144 (0.4)	1135 (0.1)	
1124 vw		1121 (1.9)	1120 (1.7)	
	1109 vw			
1098 w	1097 vw	1080 (10.3)	1077 (9.0)	
1064 w	1063 w	1075 (3.3)	1082 (3.3)	
		1048 (3.8)	1040 (1.2)	
1027 m	1025 vw	1024 (4.3)	1022 (4.3)	
1006 w	1003 w			
		992 (0.1)	996 (0.1)	
978 vw		982 (0.6)	969 (0.2)	
	976 sh	974 (3.5)	984 (3.0)	
	952 m	963 (0.6)	949 (0.2)	
	926 vw	942 (0.5)	940 (0.2)	
		906 (2.1)	903 (2.2)	
896 vw	892 sh	893 (3.5)	891 (2.0)	
	876 m	874 (0.1)	872 (0.1)	
860 vw				
	833 s	842 (18.3)	853 (17.0)	
824 m		836 (0.4)	832 (0.1)	
		792 (0.7)	790 (0.3)	
		781 (24.1)	783 (23.2)	
755 s	766 s	769 (1.5)	762 (0.2)	
730 w	735 s	747 (58.4)	744 (55.5)	
		721 (0.5)	719 (0.2)	
708 vw		713 (0.9)	719 (0.9)	

[a] Infrared intensities (in parentheses) in km/mol.
[b] Estimated uncertainties in band positions are within ±3 cm^{-1}. Relative intensities: vw = very weak, w = weak, m = medium, s = strong, vs = very strong, sh = shoulder.
[c] Unscaled DFT frequencies calculated using B3LYP/6-311+G(d,p) as described elsewhere [3].
[d] Anharmonics B3LYP/6-311 calculation using the P_VMWCl$_2$ algorithm [21,22].
[e] Eigenvector contains 5% contribution from 783 + 719 cm^{-1} combination.

consequence, predicted and observed relative intensities show only qualitative agreement in some cases.

Band frequencies in the observed spectra correspond closely to computed fundamental, combination, and overtone bands attesting to the anharmonic (mechanical and electrical) character of the vibrations. Many peaks appear in both the experimental Raman and infrared spectra, including numerous examples where the calculations, based on the behavior of individual molecules, predict activity in only one type of spectrum. This apparent disagreement, which also arises in the acene family [1,2], was resolved by performing calculations with slightly distorted molecules [37]. Small symmetry breaking distortions may arise in crystal lattices and permit bands to be both IR and Raman active.

Table 10
Raman and PA infrared spectra of 1,8-dimethylfluorene (C_{2v}), 2000–700 cm^{-1}.

Observed		Predicted[a]			
Raman[b]	Infrared[b]	Symmetry	Harmonic[c]	Anharmonic[d]	Combination[d]
	1922 m			1917(0.5)	460+1465
	1883 vw				
	1848 w				
	1775 w			1772(0.8)	780+993
	1700 w			1708(0.3)	543+1167
	1692 sh				
	1659 vw				
1602 vs		b_2	1636(1.3)	1608(0.3)	
	1592 m	a_1	1636(4.9)	1599(1.9)[e]	
		b_2	1629(14.6)	1599(5.0)	
		a_1	1626(12.7)	1590(8.2)[f]	
	1544 vw			1554(0.9)	2 × 780
		b_2	1517(0.3)	1510(0.1)	
		a_1	1515(4.5)	1503(0.1)	
		b_2	1500(34.4)	1490(15.4)	
		a_1	1497(4.0)	1485(0.2)	
1484 w	1483 sh	b_1	1488(18.3)	1465(20.7)	
		a_2	1487(0.0)	1481(0.0)	
	1452 s	b_2	1457(4.2)	1443(2.5)	
1418 w	1428 sh	a_1	1454(0.1)	1425(0.9)	
		a_1	1438(10.3)	1415(7.0)	
	1400 sh	a_1	1416(3.4)	1407(0.6)	
1380 w	1381 m	b_2	1415(0.1)	1412(0.0)	
1344 m	1344 vw	a_1	1372(0.3)	1360(0.2)	
		b_2	1343(4.2)	1337(1.0)	
	1312 m	a_1	1315(2.4)	1319(2.0)	
1292 s	1296 sh	b_2	1293(0.7)	1301(0.2)	
1260 sh	1265 vw	a_1	1265(2.7)	1253(3.1)	
1241 w	1244 vw	b_2	1248(2.9)	1251(2.8)	
	1224 vw	a_1	1212(0.7)	1200(0.2)	
		b_2	1196(1.8)	1195(1.1)	
1194 w	1196 vw	a_1	1187(1.1)	1190(0.6)	
	1175 sh	b_2	1186(0.3)	1180(0.1)	
1160 w	1159 m	a_2	1159(0.0)	1167(0.1)	
		b_2	1132(0.1)	1125(0.0)	
1113 vw	1111 vw	a_1	1100(7.3)	1101(0.9)	
		b_2	1091(5.7)	1078(3.9)	
1077 w	1073 m	b_1	1058(2.9)	1065(2.7)	
		a_2	1054(0.0)	1050(0.0)	
	1039 m	a_1	1036(0.1)	1021(0.1)	
		b_2	1006(2.1)	1000(0.2)	
1016 w		b_1	985(0.8)	993(0.6)	
	996 vw	a_2	981(0.0)	984(0.7)	
	965 vw	a_1	946(3.8)	955(1.2)	
933 m	935 vw	b_1	939(0.7)	938(0.6)	
	920 w	a_2	909(0.0)	910(0.0)	
879 vw	885 w	b_1	906(0.1)	905(0.1)	
835 m	835 vw	b_2	846(1.6)	848(0.9)	
	817 vw	a_1	845(0.0)	844(0.1)	
796 vw		a_2	810(0.0)	818(0.0)	
774 vw	768 vs	b_2	782(3.3)	775(0.9)	
749 vw	745 s	b_1	781(95.0)	780(81.2)	
724 vw		a_2	740(0.0)	730(0.0)	

[a] Infrared intensities (in parentheses) in km/mol.
[b] Estimated uncertainties in band positions are within ±3 cm^{-1}. Relative intensities: vw = very weak, w = weak, m = medium, s = strong, vs = very strong, sh = shoulder.
[c] Unscaled DFT frequencies calculated using B3LYP/6-311+G(d,p) as described elsewhere [3].
[d] Anharmonics B3LYP/6-311 calculation using the P_VMWCl$_2$ algorithm [21,22].
[e] Eigenvector contains 6% contribution from 810 + 780 cm^{-1} combination.
[f] Eigenvector contains 6% contribution from 2 × 780 cm^{-1} overtone.

Some features present in the experimental spectra, such as the 562 and 454 cm^{-1} Raman bands of fluorene and 2-ethylfluorene, respectively, appear to be absent from the computed spectra, and are also attributed to dimer effects arising in crystals. For example, the coupling of vibrations of neighboring molecules—possibly caused by pi–pi interactions—is expected to shift the frequencies of some intramolecular modes and give rise to additional features in spectra. A few additional assignments to dimer vibrations are given in the tables. Calculations of coupled vibration frequencies for condensed-ring aromatics are presently under way in our laboratory and will be reported separately.

Acknowledgements

Part of the work described in this paper was performed at the Canadian Light Source, which is supported by the Natural Sciences and Engineering Research Council of Canada, the National Research Council Canada, the Canadian Institutes of Health Research, the Province of Saskatchewan, Western Economic Diversification Canada, and the University of Saskatchewan. Computer time for this study was provided by the computing facilities MCIA (Mésocentre de Calcul Intensif Aquitain) of the Université de Bordeaux and of the Université de Pau et des Pays de l'Adour.

Appendix A. Supplementary data

Supplementary material related to this article can be found, in the online version, at http://dx.doi.org/10.1016/j.vibspec.2014.07.003.

References

[1] K.H. Michaelian, B.E. Billinghurst, J.M. Shaw, V. Lastovka, Vib. Spectrosc. 49 (2009) 28–31.
[2] K.H. Michaelian, Q. Wen, B.E. Billinghurst, J.M. Shaw, V. Lastovka, Vib. Spectrosc. 58 (2012) 50–56.
[3] N. Sallamie, J.M. Shaw, Fluid Phase Equilibr. 237 (2005) 100–110.
[4] C. Obiosa-Maife, J.M. Shaw, Energy Fuels 25 (2011) 460–471.
[5] C. Boersma, A.L. Mattioda, C.W. Bauschlicher Jr., A.G.G.M. Tielens, L.J. Allamandola, Astrophys. J. 690 (2009) 1208–1221.
[6] C. Joblin, L. d'Hendecourt, A. Léger, D. Défourneau, Astron. Astrophys. 281 (1994) 923–936.
[7] J. Szczepanski, M. Vala, Astrophys. J. 414 (1993) 646–655.
[8] C. Boersma, C.W. Bauschlicher Jr., A. Ricca, A.L. Mattioda, E. Peeters, A.G.G.M. Tielens, L.J. Allamandola, Astrophys. J. 729 (2011) 1 (14 pp.).
[9] C.W. Bauschlicher, S.R. Langhoff, Spectrochim. Acta A 53 (1997) 1225–1240.
[10] C.W. Bauschlicher Jr., Chem. Phys. 233 (1998) 29–34.
[11] C.W. Bauschlicher Jr., S.R. Langhoff, Chem. Phys. 234 (1998) 79–86.
[12] C.W. Bauschlicher Jr., Chem. Phys. 234 (1998) 87–94.
[13] C.W. Bauschlicher Jr., Chem. Phys. 262 (2000) 285–291.
[14] S.R. Langhoff, J. Phys. Chem. 100 (1996) 2819–2841.
[15] J. Oomens, G. Meijer, G. von Helden, J. Phys. Chem. A 105 (2001) 8302–8309.
[16] N. Gohaud, D. Bégué, C. Pouchan, Chem. Phys. 310 (2005) 85–96.
[17] D. Bégué, S. Elissalde, E. Pere, P. Iratcabal, C. Pouchan, J. Phys. Chem. A 110 (2006) 7793–7800.
[18] D. Bégué, P. Labéguerie, D.Y. Zhang-Negrerie, A. Avramopoulos, L. Serrano-Andrés, M.G. Papadopoulos, Phys. Chem. Chem. Phys. 12 (2010) 13746–13751.
[19] D. Bégué, I. Baraille, P.-A. Garrain, A. Dargelos, T. Tassaing, J. Chem. Phys. 133 (2010) 034102 (13 pp.).
[20] D. Bégué, G.G. Qiao, C. Wentrup, J. Am. Chem. Soc. 134 (2012) 5339–5350.
[21] I. Baraille, C. Larrieu, A. Dargelos, M. Chaillet, Chem. Phys. 273 (2001) 91–101.
[22] D. Bégué, N. Gohaud, C. Pouchan, P. Cassam-Chenai, J. Liévin, J. Chem. Phys. 127 (2007) 164115 (10 pp.).
[23] M. Abo-Bakr, J. Feikes, K. Holldack, P. Kuske, W.B. Peatman, U. Schade, G. Wüstefeld, H.-W. Hübers, Phys. Rev. Lett. 90 (2003) 094801 (4 pp.).
[24] B. Billinghurst, T. May, L. Dallin, W. Wurtz, M. de Jong, K.H. Michaelian, Opt. Lett. 35 (2010) 3090–3092.
[25] J.M. Hume, G.I. Jenkins, Appl. Spectrosc. 18 (1964) 161–166.
[26] A. Bree, R. Zwarich, J. Chem. Phys. 51 (1969) 912–920.
[27] S.Y. Lee, B.Y. Boo, J. Phys. Chem. 100 (1996) 8782–8785.
[28] T. Thormann, M. Rogojerov, B. Jordanov, E.W. Thulstrup, J. Mol. Struct. 509 (1999) 93–104.
[29] C.R. Johnson, S.A. Asher, Anal. Chem. 56 (1984) 2258–2261.
[30] R. Rumelfanger, S.A. Asher, M.B. Perry, Appl. Spectrosc. 42 (1988) 267–272.
[31] Y.T. Chua, P.C. Stair, J. Catal. 213 (2003) 39–46.
[32] D.S. Cordeiro, P. Corio, J. Braz. Chem. Soc. 20 (2009) 80–87.
[33] S. Chakraborty, P. Das, S. Manogaran, P.K. Das, Vibr. Spectrosc. 68 (2013) 162–169.
[34] J. Banisaukas, J. Szczepanski, M. Vala, S. Hirata, J. Phys. Chem. A 108 (2004) 3713–3722.
[35] Q. Wen, K.H. Michaelian, Opt. Lett. 33 (2008) 1875–1877.
[36] M. Dehghany, K.H. Michaelian, Rev. Sci. Instrum. 83 (2012) 064901 (4 pp.).
[37] F. Spillebout, D. Bégué, I. Baraille, J.M. Shaw, Energy Fuels 28 (2014) 2933–2947.